

# Stimulated electromagnetic emissions and anomalous HF wave absorption near electron gyroharmonics

P. Stubbe

Max-Planck-Institut für Aeronomie, Katlenburg-Lindau, Germany

A. J. Stocker, F. Honary, T. R. Robinson, and T. B. Jones

Department of Physics and Astronomy, Leicester University, Leicester, United Kingdom

**Abstract.** Simultaneous observations are presented of stimulated electromagnetic emission (SEE) spectra and the anomalous absorption of a diagnostic HF wave, caused by powerful radio waves generated by the Tromsø heating facility. The pump frequency was varied in small steps around the third, fourth, and fifth harmonic of the electron gyrofrequency. Systematic variations with pump frequency were observed in the anomalous absorption data and the entirety of SEE properties. The anomalous absorption exhibits a pronounced minimum at a certain pump frequency near (or at) the gyroharmonic in question. Of the SEE properties the strength and discreteness of the downshifted maximum and the width of the downshifted continuum minimize together with the anomalous absorption. Other SEE properties (namely the broad upshifted maximum, the downshifted peak, and the broad symmetrical structure) exist only in well-defined narrow pump frequency ranges near the absorption minimum. Significant quantitative and qualitative differences are found between the SEE properties around the third gyroharmonic on the one hand, and the fourth and fifth gyroharmonics on the other hand.

## 1. Introduction

A powerful electromagnetic wave (with angular frequency  $\omega_0$ ), incident upon the ionospheric plasma, may generate secondary electromagnetic waves at frequencies approximately ranging from  $0.98 \omega_0$  to  $1.04 \omega_0$ . This phenomenon, termed stimulated electromagnetic emission (SEE), was discovered in ionospheric modification experiments at Tromsø, Norway, in 1981. First experimental results were reported by *Thidé et al.* [1982], and a classification of the main SEE characteristics was given by *Stubbe et al.* [1984].

The excitation of SEE requires an *O*-mode pump wave with a frequency below the maximum *F* region plasma frequency. There is no other constraint on the pump frequency  $\omega_0$ . It has been found, however, that the character of the SEE spectra changes strongly when  $\omega_0$  approaches an integer multiple of the electron gyrofrequency,  $\omega_0 \approx n\Omega_e$  [*Leysner et al.*, 1990]. Whereas some of the SEE features become particularly strong or weak when  $\omega_0$  is changed in small steps ( $\sim 2\pi \times 10$  kHz) around  $n\Omega_e$ , others exist only when the condition  $\omega_0 \approx n\Omega_e$  is met.

This experimental finding most naturally points to the importance of electron Bernstein waves for the SEE phenomenon. High-frequency electrostatic waves propagating perpendicular to the external magnetic field are thought to be generated by linear mode conversion of the electromagnetic pump wave at small-scale field-aligned density irregularities, so-called striations [*Mjølhus*, 1990, and references therein]. The same striations are also thought to be responsible for the anomalous absorption imposed upon an *O*-mode wave prop-

agating through an ionospheric volume affected by the pump wave [*Graham and Fejer*, 1976]. Naturally, the pump itself is also subject to this anomalous absorption, giving rise to a self-absorption effect.

The phenomenon of anomalous HF wave absorption (or wideband attenuation, as it was called previously) has been discovered in ionospheric modification experiments performed near Boulder, Colorado [e.g., *Utlaut and Violette*, 1974]. This phenomenon has also been the research subject in a series of experiments conducted at Tromsø in which several new features were found [*Stubbe et al.*, 1982; *Kopka et al.*, 1982; *Jones et al.*, 1983, 1984]. In these earlier experiments, systematic pump frequency changes in small steps around  $n\Omega_e$  were not made, and simultaneous SEE experiments not performed.

Combined anomalous absorption and SEE measurements, involving systematic pump frequency changes around  $n\Omega_e$ , have been performed at Tromsø in three special campaigns in May 1991, August 1991, and October 1992. A total of 75 hours of heater operation has been invested in these experiments. Results from these three campaigns will be presented and discussed subsequently. A selection of anomalous absorption results from the May and August 1991 campaigns were presented by *Stocker et al.* [1993], where it was shown that the anomalous absorption goes through a distinct minimum as the pump frequency passes through  $n\Omega_e$ .

## 2. Experimental Arrangement

A detailed description of the experimental arrangement has been given by *Stocker et al.* [1993] and does not need to be repeated here. In short, the experiments involve four

Copyright 1994 by the American Geophysical Union.

Paper number 94JA00023.  
0148-0227/94/94JA-00023\$05.00

manually operated stations. (1) At the Heating Station a powerful electromagnetic  $O$ -mode wave is radiated vertically into the ionosphere. Its frequency is changed in small steps around  $n\Omega_e$  ( $n = 3, 4, 5$ ), where  $\Omega_e \approx 2\pi \times 1.35$  MHz. A typical residence time on a given frequency, including some off/on switching, is 6 min, a typical tuning time to a new frequency is 2 min, and a typical frequency increment is 10 or 20 kHz. (2) At the North Station (50 km to the north of the heater), four HF transmitters are employed to radiate diagnostic waves on four different frequencies obliquely into the modified  $F$  region. Usually, two of the four frequencies are kept fixed, and two frequencies are sliding with the pump frequency; that is, they differ from the pump frequency by a fixed amount. (3) The corresponding HF receivers are located at the South Station (45 km to the south of the heater). One additional receiver is used to monitor the ionospherically reflected pump wave. From these data the anomalous absorption of the diagnostic waves and the pump wave may be derived. (4) The East Station (17 km to the east of the heater) contains the equipment for real time recording of SEE spectra. These spectra are also used as a basis for determining the pump frequency range to be scanned in the experiments. One complete frequency scan takes 1.5 to 2.5 hours; stable ionospheric conditions are therefore required in these experiments.

### 3. Experimental Results

The experimental results will be presented in two parts. In section 3.1, anomalous absorption as a function of pump frequency will be shown in conjunction with selected SEE spectra, taken at some of these pump frequencies. In section 3.2 a more systematic comparison will be made by extracting a few key parameters from the SEE spectra and presenting them, again together with anomalous absorption data, as a function of pump frequency. In this way, very characteristic changes with pump frequency and interdependencies between different data sets will be revealed, providing a unique information base to guide theoretical work.

#### 3.1. Anomalous Absorption and SEE Spectra

Anomalous absorption data and SEE spectra are shown in Figure 1 for  $n = 5$  (i.e., for pump frequencies around the fifth harmonic of the electron gyrofrequency), in Figure 2 for  $n = 4$ , and in Figure 3 for  $n = 3$ . Data points for which corresponding SEE spectra are presented in the same figure are marked by small letters. Two spectra are shown for each case, differing with respect to frequency span, in order to highlight different spectral portions. The spectral features to be noted are the "continuum," the "downshifted maximum" (DM), the "broad upshifted maximum" (BUM), the "downshifted peak" (DP), and the "broad symmetrical structure" (BSS).

The continuum is a continuous spectrum appearing on both sides of the pump frequency  $f_0$ , with a peak at  $f_0$ . The continuum is usually asymmetric, with more spectral energy on the downshifted side. The width of the downshifted part of the continuum is strongly variable, ranging from a few kilohertz up to as much as 100 kHz. Examples of a strongly developed continuum are seen in Figure 1 (panels a and e).

The DM is a spectral maximum occurring at a frequency offset from the pump approximately given by  $\Delta f_{DM} = -2 \times 10^{-3} f_0$ , with a width of a few kilohertz [Stubbe et al.,

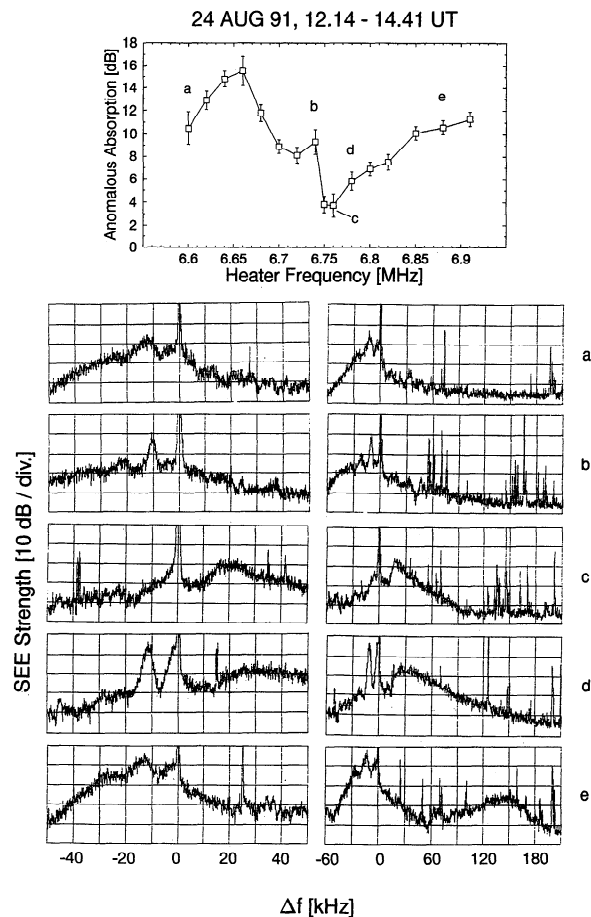


**Figure 1.** Experimental results obtained on August 24, 1991, from 1214 to 1441 UT for pump frequencies around the fifth gyroharmonic. The heater was operated in  $O$  mode, with an effective radiated power (ERP) of 230 MW. (Upper) Anomalous absorption of a diagnostic wave with frequency 70 kHz below pump frequency, as a function of pump frequency. (a–e): SEE spectra, belonging to the pump frequencies marked in the upper panel. Shown is the SEE strength in relative units (10 dB/division) versus frequency offset  $\Delta f \equiv f - f_0$ . The strong maximum at  $\Delta f = 0$  corresponds to the totally reflected pump wave. Two spectra are presented for each of the selected pump frequencies, differing with regard to frequency span. The left-sided spectra cover the frequency range  $-50$  to  $50$  kHz, and the right-sided spectra cover the frequency range  $-60$  to  $210$  kHz, relative to the pump frequency. Notice that the spiky peaks in the spectra are due to interfering radio stations.

1984]. Like the continuum, the DM has a highly variable shape. In one extreme the DM appears as a slightly elevated portion within a broad downshifted continuum (e.g., Figure 1, panels a and e). In the other extreme the DM is sharply peaked, looking like the copy of an equally sharp continuum (e.g., Figure 1, panel d). A necessary condition for the latter to occur is that the pump frequency is close to a gyroharmonic. A strongly developed DM is often accompanied by a maximum at twice the offset frequency of the DM, called the 2DM (e.g., Figure 2, panel b). Occasionally, a 3DM feature is observed [Stubbe et al., 1984] but not in the results shown in the present paper.

The BUM is a feature that exists exclusively on the

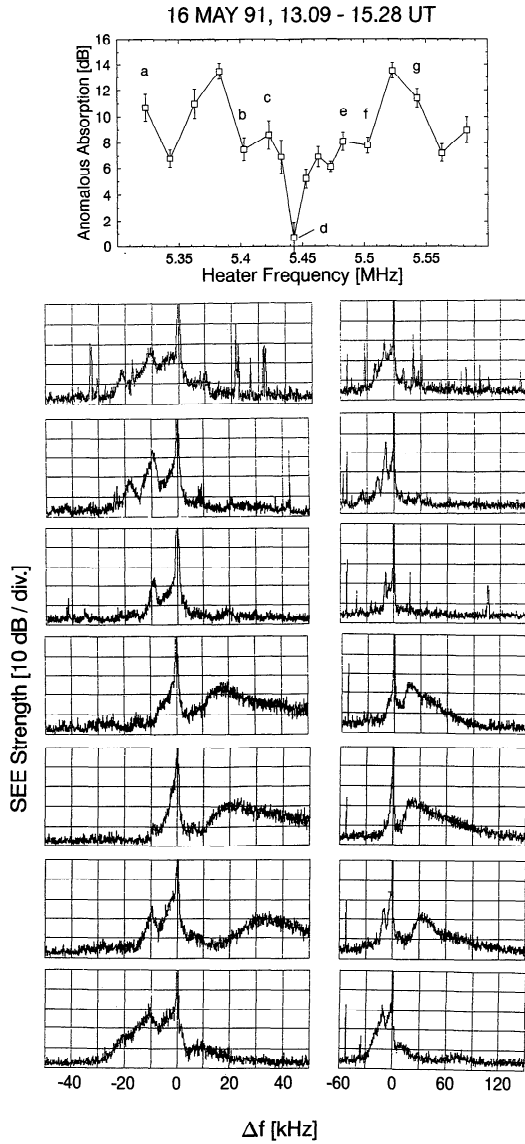


**Figure 2.** Experimental results obtained on May 16, 1991, from 1309 to 1528 UT for pump frequencies around the fourth gyroharmonic. The heater was operated in *O* mode, with an ERP of 210 MW. (Upper) Anomalous absorption of a diagnostic wave with frequency 53 kHz below pump frequency, as a function of pump frequency. (a–g) SEE spectra, belonging to the pump frequencies marked in the upper panel. Two spectra are presented for each of the select, differing with regard to frequency span. The left-sided spectra cover the frequency range  $-50$  to  $50$  kHz, and the right-sided spectra cover the frequency range  $-60$  to  $150$  kHz, relative to the pump frequency. Further text as in Figure 1.

upshifted side and may reach out to  $\Delta f = 200$  kHz, or even more. The peak frequency depends strongly on  $f_0$  and can be approximated by  $\Delta\omega_{\text{BUM}} = \omega_0 - n\Omega_e$  [Leyser et al., 1990]. When  $f_0$  is lowered so that  $\Delta f_{\text{BUM}}$  approaches zero, the BUM begins to disappear and ceases to exist below approximately 15 kHz. Examples of a well developed BUM are seen in Figure 1 (panels c–e) and Figure 2 (panels d–f).

The DP is the spectral peak nearest to  $f_0$ , with  $\Delta f_{\text{DP}}$  falling into the range  $-3$  to  $-1$  kHz. The DP is a well developed

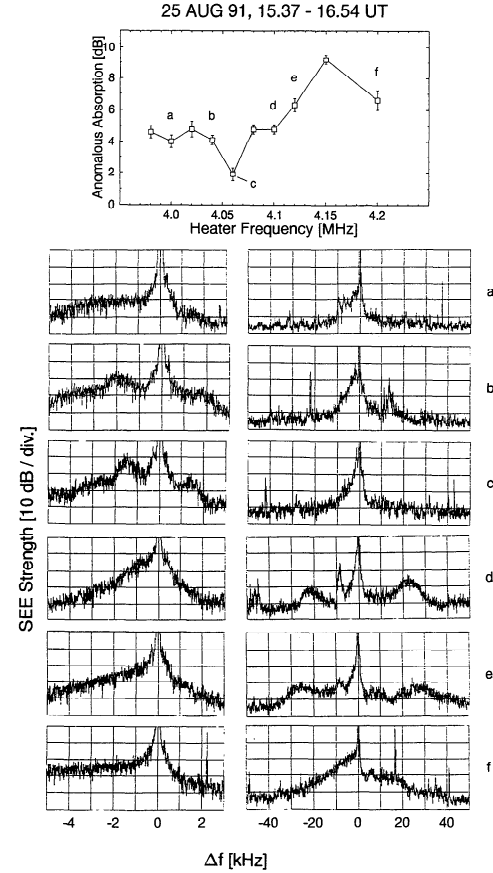


**Figure 3.** Experimental results obtained on August 25, 1991, from 1537 to 1654 UT for pump frequencies around the third gyroharmonic. The heater was operated in *O* mode, with an ERP of 210 MW. (Upper) Anomalous absorption of a diagnostic wave with frequency 70 kHz below pump frequency, as a function of pump frequency. (a–f) SEE spectra, belonging to the pump frequencies marked in the upper panel. Two spectra are presented for each of the selected pump frequencies, differing with regard to frequency span. The left-sided spectra cover the frequency range  $-5$  to  $3$  kHz, and the right-sided spectra cover the frequency range  $-50$  to  $50$  kHz, relative to the pump frequency. Further text as in Figure 1.

feature only for  $n = 3$ . Only weak signs of a DP have been seen for  $n = 4$  and  $n = 5$ , and none for  $n = 6$ , despite systematic searches. The DP is clearly shown in Figure 3 (panels b and c).

The BSS is the only SEE feature that may exist in an almost perfectly symmetric form. In its fully developed state the BSS consists of two broad maxima at  $\Delta f_{\text{BSS}} \approx \pm 30$  kHz [Stubbe and Kopka, 1990]. The BSS has only been observed for pump frequencies falling into an extremely narrow frequency range ( $\sim 40$  kHz) near the third gyroharmonic. The BSS has not been found for  $n = 4$  to  $6$  and is as such complementary to the BUM, which is well developed for  $n = 4$  to  $6$  but not for  $n = 3$ . In another sense the BSS is complementary to the DP: When the pump frequency is chosen such that a DP exists and is then increased in small steps, the DP will, at some pump frequency, cease to exist, while at the same frequency the BSS will begin to exist. An example of the BSS is shown in Figure 3 (panels d and e).

With these introductory remarks in mind, we will now look through Figures 1 to 3. In Figure 1, pertaining to  $n = 5$ , we see that the absorption has a maximum at 6.66 MHz, and a minimum at 6.75 to 6.76 MHz. On the way from point a to point b, only small changes occur in the SEE spectra. The continuum becomes slightly weaker, and the DM somewhat sharper. Drastic changes occur, however, when we go on from point b to d, i.e., from  $f_0 = 6.74$  to  $f_0 = 6.78$  MHz. At the intermediate point c, the DM disappears completely, while the BUM appears as a new feature. At point d, only 20 kHz higher in frequency, the DM has not only reappeared, but has adopted a very high value and discrete shape. On going further to point e, the continuum has recovered, and the BUM has moved to higher frequencies (before disappearing at still higher pump frequencies). It is clear from this comparison that the absorption changes taking place around the absorption minimum are accompanied by pronounced changes in the SEE spectra. The same does not hold true for the absorption maximum, and it is questionable therefore whether this maximum is a significant feature. Indeed, other absorption measurements for the case  $n = 5$  have not confirmed the existence of a reproducible maximum at frequencies below the absorption minimum.

The case  $n = 4$ , depicted by Figure 2, is very similar to the case  $n = 5$ . The only obvious difference is that the BUM exists in a much narrower range of  $\Delta f$ . Again, it is seen that the absorption minimum (at  $f_0 = 5.44$  MHz) coincides with characteristic changes in the SEE spectra, including a disappearance and strong reappearance of the DM.

A largely different situation is found for  $n = 3$ , as seen in Figure 3. The DP and the BSS occur as new features, whereas the BUM no longer exists. We notice that the anomalous absorption possesses a minimum (at  $f_0 = 4.06$  MHz) and a maximum (at  $f_0 = 4.15$  MHz). At point a a weak DP shows up at  $\Delta f_{DP} \approx -3$  kHz, and the DM occurs in split form (i.e., the DM consists of two maxima, separated by approximately 2.5 kHz). A split DM has been found in our experiments to be a characteristic feature for pump frequencies near the third gyroharmonic. At points b and c the DP has sharpened and moved toward smaller offset frequencies, whereas the DM has disappeared. At point d, to the right of the absorption minimum, the DP is vanishing in the continuum (and is barely visible at  $\Delta f_{DP} \approx -0.9$  kHz). Simultaneously, the BSS appears, and the DM reoccurs in a very pronounced form. At point e the BSS has reached its highest peak frequency  $\Delta f_{BSS} \approx \pm 30$  kHz, and disappears for slightly higher pump frequencies. The DM is now much less pronounced, and vanishes in the continuum at point f. The absorption maximum, occurring to the right of the absorption minimum, is a significant feature (unlike the absorption maximum seen in Figure 1), since it has been found in all experiments around the third gyroharmonic.

We have also performed a few experiments with a larger pump frequency increment, in order to investigate the changes that take place between gyroharmonics. One such case is shown in Figure 4. Here only one spectrum per chosen pump frequency is presented, since the DP and BUM do not exist outside the gyroharmonics range, so that special frequency span settings are not required. We see that between gyroharmonics the downshifted portion of the continuum is the dominating feature in the SEE spectra. The absorption shows a very pronounced maximum at  $f_0 = 4.2$ – $4.3$  MHz, reaching up to 27 dB. These are the highest absorption values ever found. Another feature worthy of

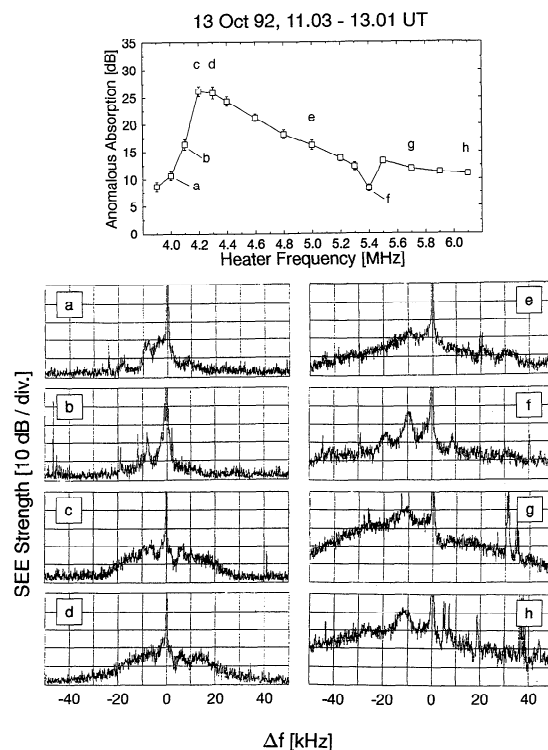


**Figure 4.** Experimental results obtained on October 13, 1992, from 1103 to 1301 UT for pump frequencies ranging from 3.9 to 6.3 MHz. The heater was operated in *O* mode, with an ERP of 230 MW. (Upper) Anomalous absorption of a diagnostic wave with frequency 70 kHz below pump frequency, as a function of pump frequency. (a–h) SEE spectra, belonging to the pump frequencies marked in the upper panel, covering the frequency range  $-50$  to  $50$  kHz, relative to the pump frequency. Further text as in Figure 1.

being noted is a significant increase in overall spectral strength when we pass through the fourth gyroharmonic toward higher pump frequencies. For instance, the strength of the DM increases by approximately 20 dB when passing the fourth gyroharmonic.

### 3.2. Anomalous Absorption and SEE Spectral Parameters

In order to get a more concise comparison of absorption and spectral measurements, we will now proceed to extract certain key parameters from the SEE spectra and compare them with the absorption data (and with each other). We have chosen the following parameters:

1. The strength of the downshifted maximum, measured from the basis line (which is approximately the noise level). This parameter will be labeled “DM” in the following figures. If a developed maximum does not exist, the spectral strength is measured at the frequency where the downshifted maximum should be expected.
2. The strength of the downshifted maximum, measured from the right-sided continuum. This parameter will be labeled “(DM)”, and it may be taken as a measure of the discreteness of the downshifted maximum. A large value of (DM), in conjunction with a small difference between DM and (DM), indicates that the downshifted maximum is shaped like a discrete spectral line.
3. The spectral strength at twice the offset frequency of the downshifted maximum (measured from the basis line).

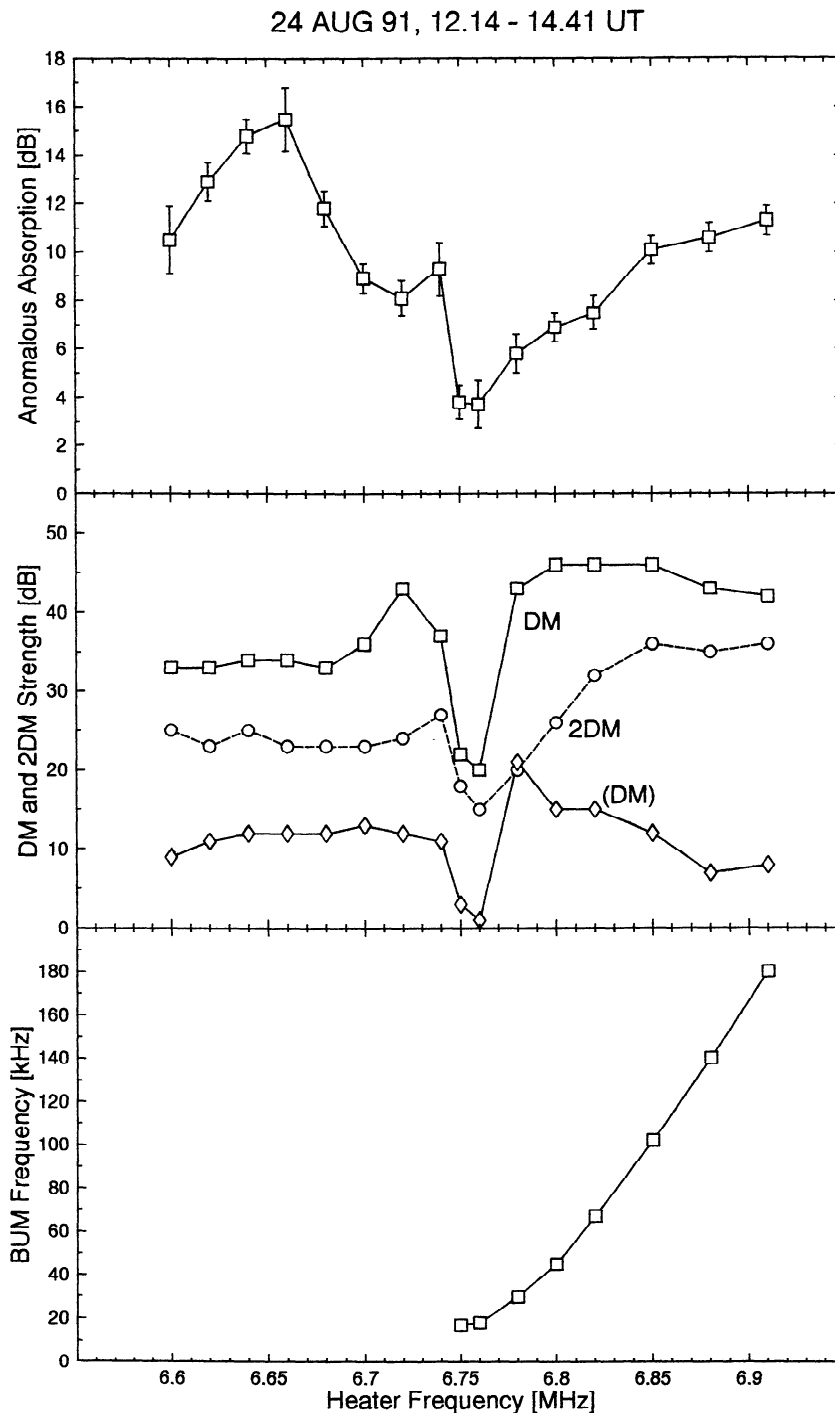


**Figure 5.** Experimental results obtained on August 24, 1991, from 1214 to 1441 UT for pump frequencies around the fifth gyroharmonic. The heater was operated in *O* mode, with an ERP of 230 MW. (Upper) Anomalous absorption of a diagnostic wave with frequency 70 kHz below pump frequency, as a function of pump frequency. (Middle) Characteristic spectral properties, as defined in section 3.2 under points 1–3, as a function of pump frequency. (Lower)  $\Delta f_{\text{BUM}}$  as a function of pump frequency.

This parameter will be labeled “2DM,” and it may be taken as a measure of the width of the downshifted SEE spectrum. A large value of 2DM, in conjunction with a small difference between DM and 2DM, indicates a wide spectrum. This parameter will not be used for  $n = 3$ , since the spectral intensity at  $2\Delta f_{\text{DM}}$  is usually very small in this case.

4. The frequency of the BUM,  $\Delta f_{\text{BUM}}$ . This parameter will be used for the cases  $n = 4$  and  $n = 5$  only.

5. The strength of the DP, measured from the basis line. This parameter will be used for the case  $n = 3$  only.

6. The frequency of the DP,  $\Delta f_{\text{DP}}$ . This parameter, too, will be used for the case  $n = 3$  only.

Results for the case  $n = 5$  are presented in Figures 5–7. These figures show that the spectral properties vary in a more regular fashion than the absorption data. There is a very obvious agreement between the absorption minimum

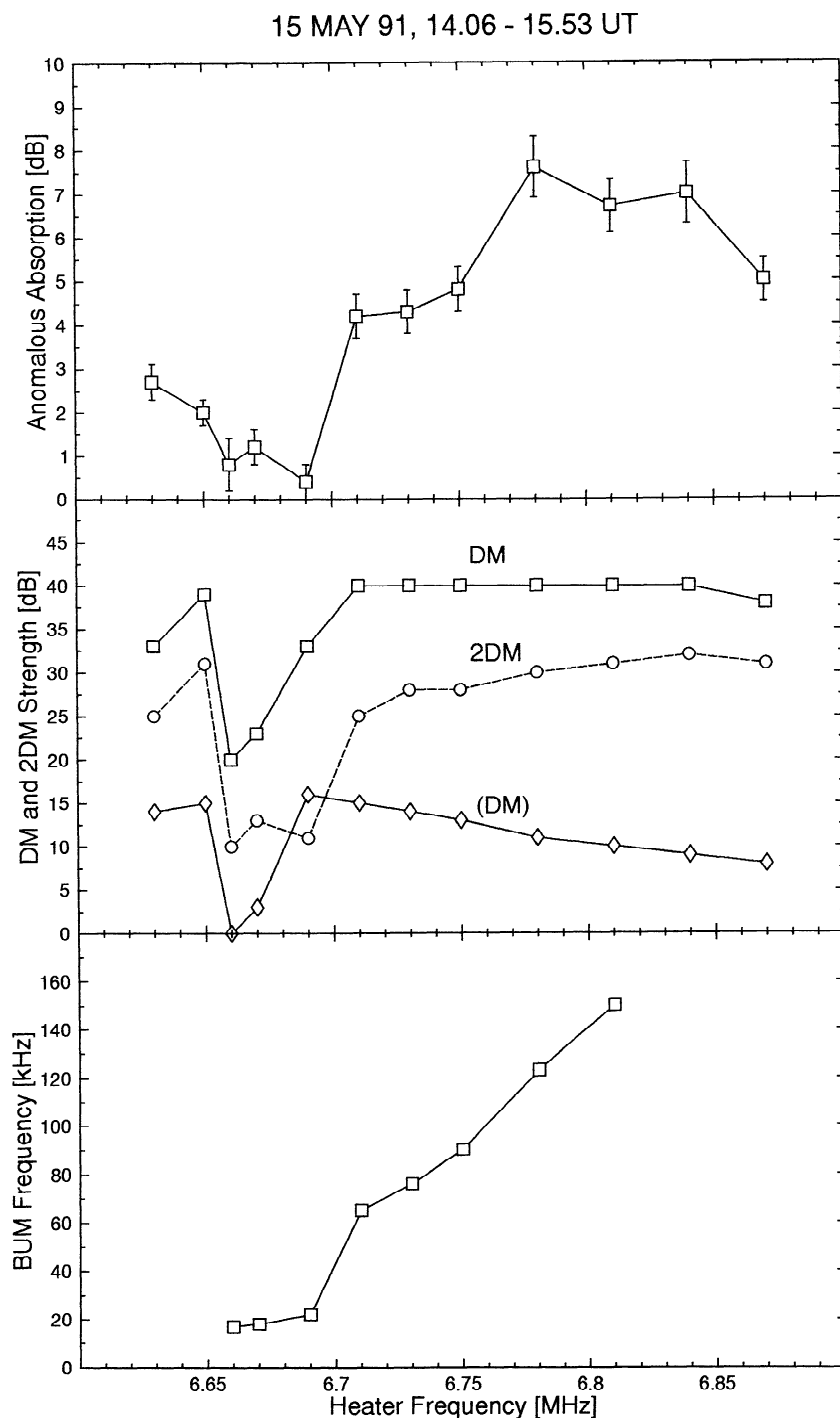


**Figure 6.** Experimental results obtained on May 15, 1991, from 1406 to 1553 UT for pump frequencies around the fifth gyroharmonic. The heater was operated in *O* mode, with an ERP of 770 MW. (Upper) Anomalous absorption of a diagnostic wave with frequency 50 kHz below pump frequency, as a function of pump frequency. Further text as in Figure 5.

and corresponding minima in the DM, (DM), and 2DM curves. A closer inspection shows that the absorption minimum consists of two parts, a sharp minimum which agrees well with corresponding minima in DM and (DM), and a wide minimum (of which the sharp minimum is a part) which agrees well with a corresponding minimum in 2DM. The sharp absorption minimum is thus accompanied by a weak downshifted SEE spectrum in general and the absence of a

downshifted maximum in particular. The wide absorption minimum is accompanied by a narrow downshifted SEE spectrum. The behavior of the BUM reflects very clearly the variations that occur in the other quantities: The BUM starts to exist at the sharp absorption minimum. The curve  $\Delta f_{\text{BUM}}$  versus  $f_0$  has a small slope inside the wide absorption minimum, and a large slope beyond the wide minimum. The transition from a small to a large slope coincides with a

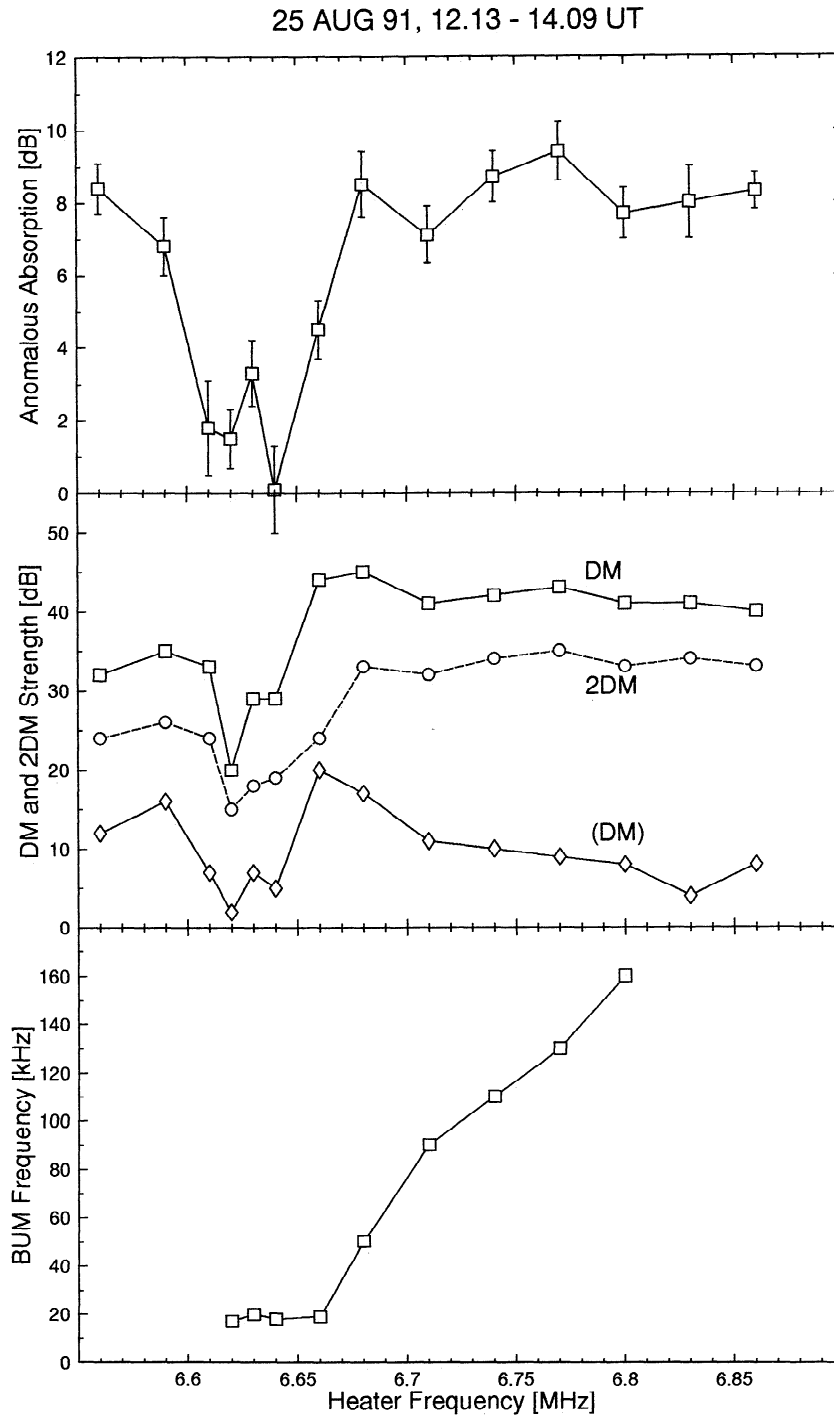


**Figure 7.** Experimental results obtained on August 25, 1991, from 1213 to 1409 UT for pump frequencies around the fifth gyroharmonic. The heater was operated in *O* mode, with an ERP of 210 MW. (Upper) Anomalous absorption of a diagnostic wave with frequency 70 kHz below pump frequency, as a function of pump frequency. Further text as in Figure 5.

maximum in the discreteness of the downshifted maximum, as shown by the (DM) curve.

Corresponding results for the case  $n = 4$  are presented in Figure 8. These data show properties very similar to those for  $n = 5$ . One noteworthy difference is that the discreteness of the downshifted maximum, indicated by the curve labeled “(DM)”, maximizes at pump frequencies below the absorption minimum for  $n = 4$ , and above the absorption minimum

for  $n = 5$ . Moreover, it is seen that the pump frequency range in which the BUM exists is much wider for  $n = 5$  than for  $n = 4$ .

Again, the situation is largely different for the case  $n = 3$ , as seen from Figures 9 and 10. In the lower panel of these figures, the DP strength and DP frequency are shown now (instead of the BUM frequency), and in the upper panel the occurrence of a split DM and of a BSS is indicated. The

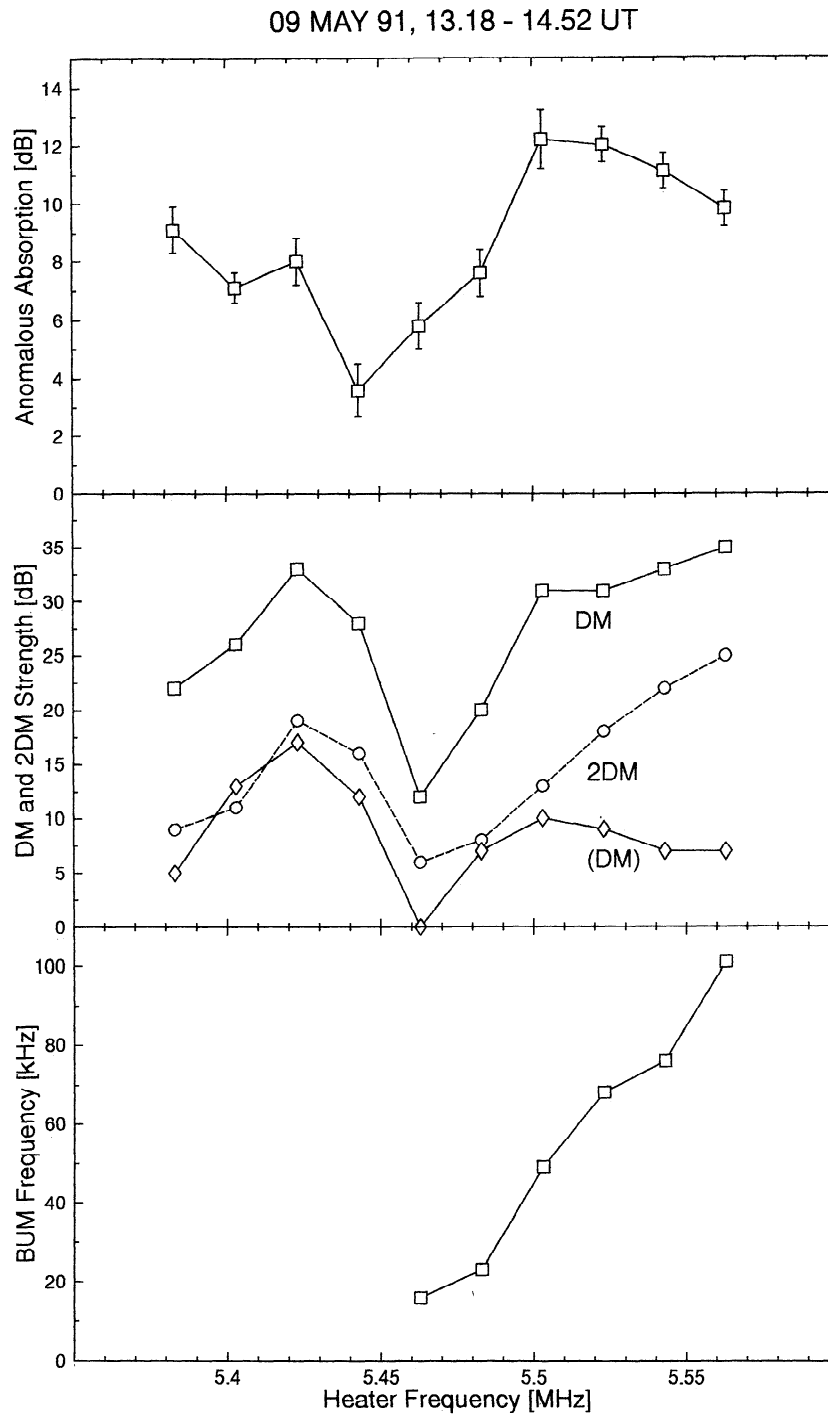


**Figure 8.** Experimental results obtained on May 9, 1991, from 1318 to 1452 UT for pump frequencies around the fourth gyroharmonic. The heater was operated in *O* mode, with an ERP of 210 MW. (Upper) Anomalous absorption of a diagnostic wave with frequency 63 kHz below pump frequency, as a function of pump frequency. Further text as in Figure 5.

absorption minimum, and even more so the minimum in DM, are less clearly pronounced here than for  $n = 4$  and  $n = 5$ . As a strongly pronounced new feature, an absorption maximum is showing up approximately 80 kHz above the absorption minimum. The discreteness of the downshifted maximum, indicated by the (DM) curve, has a well-developed maximum to the right of the absorption minimum. The BSS starts to exist just at this maximum, whereas the

split DM occurs at frequencies well below the absorption minimum. The DP exists mainly at frequencies below the absorption minimum, and its maximum strength coincides with the absorption minimum. The DP ceases to exist at, or slightly to the left of, the (DM) maximum and the BSS range of existence.

The frequency range of interest, that is, the range of pump frequencies in which the characteristic changes discussed



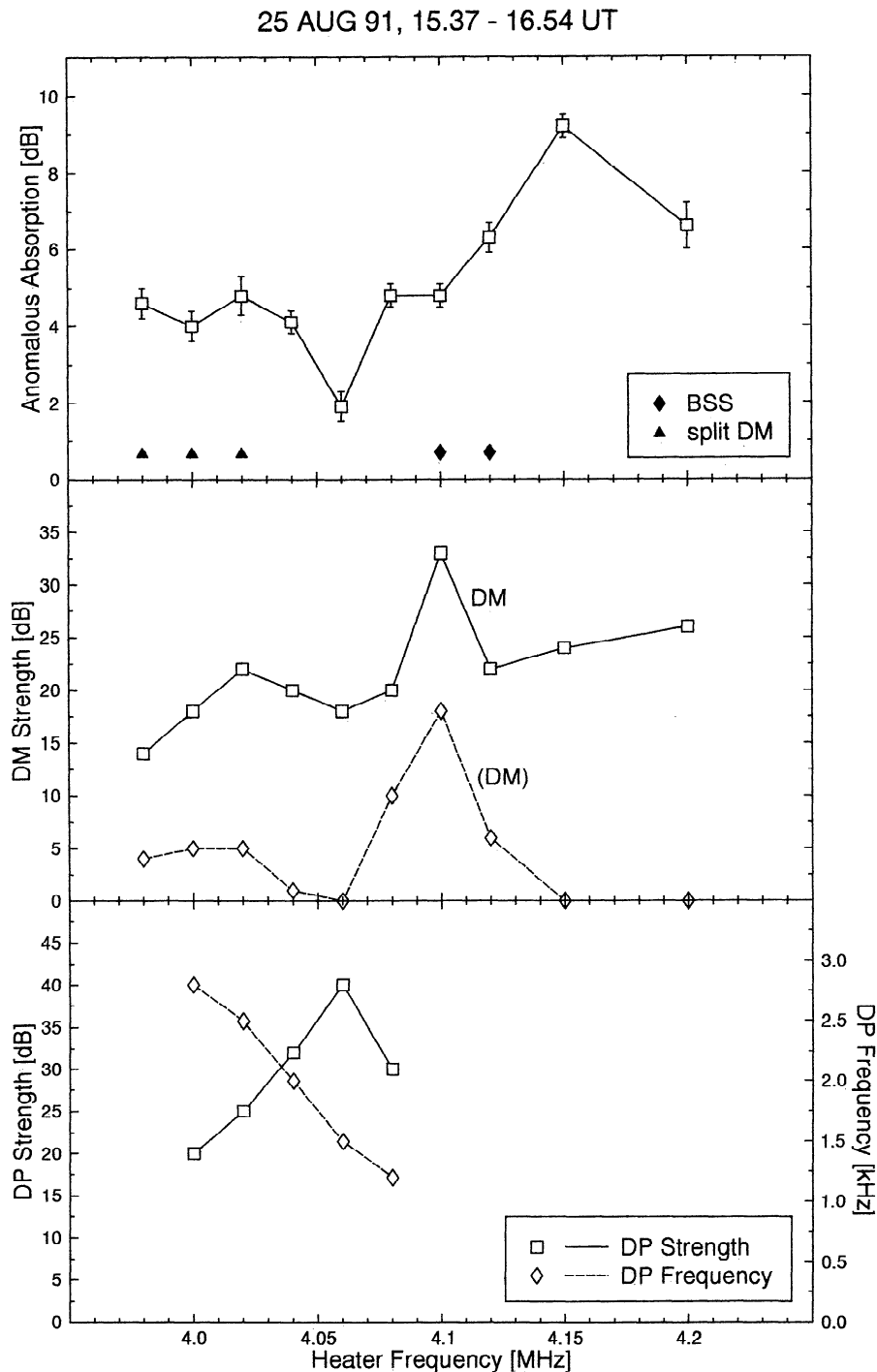


**Figure 9.** Experimental results obtained on August 25, 1991, from 1537 to 1654 UT for pump frequencies around the third gyroharmonic. The heater was operated in *O* mode, with an ERP of 210 MW. (Upper) Anomalous absorption of a diagnostic wave with frequency 70 kHz below pump frequency, as a function of pump frequency. The occurrence of a split DM and of a BSS is indicated by triangles and diamonds, respectively. (Middle) Characteristic spectral properties, as defined in section 3.2 under points 1 and 2, as a function of pump frequency. (Lower) DP strength (measured from the basis line) and DP frequency,  $|\Delta f_{DP}|$ , as a function of pump frequency.

above are taking place, spans approximately 200 kHz. The electron gyrofrequency in the interaction region (where the physical processes giving rise to the observed features occur) is known sufficiently well to warrant the statement that this frequency range of interest includes the gyrohar-

monic in question. It is not possible, however, to connect any particular absorption or spectral feature precisely to the respective gyroharmonic. This will have to be left to a thorough theoretical analysis of the problems at hand.

The heating facility near Tromsø, in its present form,

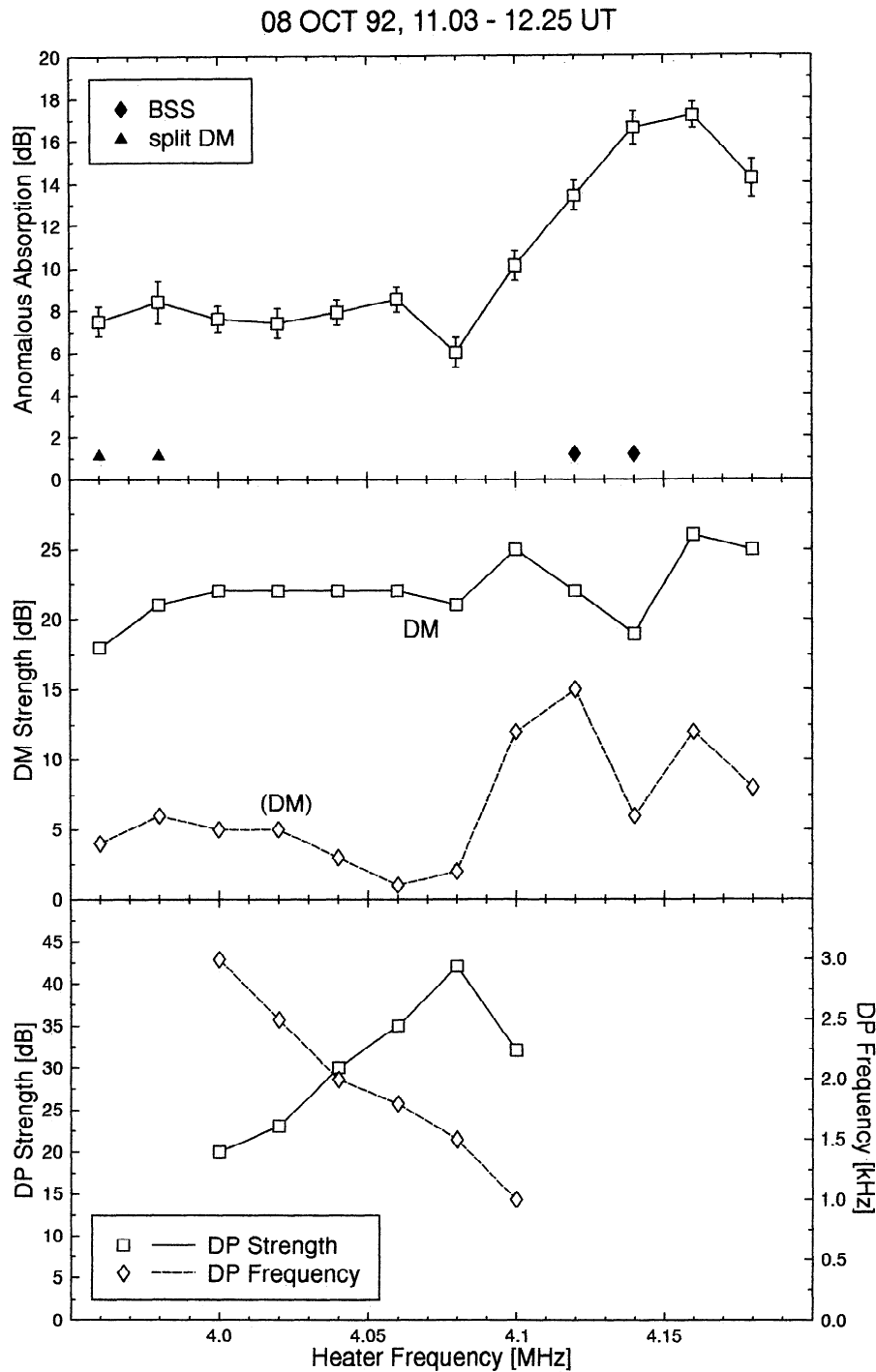


**Figure 10.** Experimental results obtained on October 8, 1992, from 1103 to 1225 UT for pump frequencies around the third gyroharmonic. The heater was operated in *O* mode, with an ERP of 230 MW. (Upper) Anomalous absorption of a diagnostic wave with frequency 70 kHz below pump frequency, as a function of pump frequency. Further text as in Figure 9.

covers the gyroharmonics from  $n = 3$  to  $n = 6$ . The reason that results for  $n = 6$  were not obtained in the experiments reported here is that the critical *F* region frequency never reached up to the sixth gyroharmonic. From previous SEE experiments it is known, however, that the case  $n = 6$  extends the cases  $n = 4$  and 5. This implies that the pump frequency range in which the BUM exists and the spectral width of the BUM increase when we step up from  $n = 4$  via

$n = 5$  to  $n = 6$ . As for the cases  $n = 4$  and  $n = 5$ , the DP and BSS do not exist for  $n = 6$ .

#### 4. Summary and Discussion

The experimental results presented in section 3 show an immense complexity. The basic findings are summarized as follows.

1. Characteristic changes occur in the anomalous absorption of an  $O$ -mode HF wave and in the properties of stimulated electromagnetic emission (SEE) spectra when the pump frequency is changed in small steps around an integer multiple of the electron gyrofrequency,  $\omega_0 \approx n\Omega_e$ .

2. While some of the SEE features (continuum, DM, 2DM) undergo strong changes when  $\omega_0$  is changed around  $n\Omega_e$ , other SEE features (BUM, DP, BSS), in addition to experiencing strong changes, exist only when the condition  $\omega_0 \approx n\Omega_e$  is satisfied.

3. There are characteristic differences between the case  $n = 3$  on the one hand, and  $n = 4$  or  $5$  on the other hand. The BUM is a well-developed feature for  $n = 4$  or  $5$  (and also for  $n = 6$ ), but not for  $n = 3$ . On the other hand, the DP and BSS are well-developed features for  $n = 3$ , but not for  $n = 4$  or  $5$  (and  $n = 6$ ).

4. The anomalous absorption possesses a minimum near (or possibly at)  $\omega_0 = n\Omega_e$ . This absorption minimum is accompanied by a minimum in the strength and discreteness of the DM and by a minimum in the width of the downshifted SEE spectrum.

5. The discreteness of the DM has a sharp maximum at a pump frequency below the absorption minimum for the case  $n = 4$  and above the absorption minimum for the cases  $n = 3$  and  $n = 5$ .

6. Between gyroharmonics, the SEE spectra are dominated by the downshifted continuum.

Other experimental findings of a more detailed kind are the following:

7. For the case  $n = 5$  the absorption minimum consists of two parts, namely, a sharp and a wide minimum. The first forms the left edge of the latter. The sharp minimum agrees well with the corresponding minimum in the strength and the discreteness of the DM. The wide minimum agrees well with the minimum in the width of the downshifted SEE spectrum.

8. The BUM starts to exist at the pump frequency of the left edge of the absorption minimum (i.e., at the sharp absorption minimum in the case  $n = 5$ ). Inside the absorption minimum, the slope of the curve  $\Delta f_{\text{BUM}}$  versus  $\omega_0$  is small, sometimes close to zero. At pump frequencies above the absorption minimum the slope increases sharply, and  $\Delta f_{\text{BUM}}$  can now reasonably well be described by the function  $\omega_0 - n\Omega_e$ . These statements refer to the cases  $n = 4$  and  $n = 5$ .

9. The DP exists mainly at pump frequencies below the absorption minimum. Its maximum strength coincides with the absorption minimum. The BSS exists at pump frequencies above the absorption minimum. The BSS starts to exist at the pump frequency of the maximum of the DM discreteness. These statements refer to the case  $n = 3$ .

10. For the case  $n = 3$  the DM may occur in split (i.e., doubly peaked) form, at pump frequencies below the absorption minimum.

11. For the case  $n = 3$  the anomalous absorption possesses a maximum at a pump frequency approximately 80 kHz above the absorption minimum. Extremely high values of the anomalous absorption (up to 27 dB) have been found at the maximum. No systematically occurring absorption maxima have been found around the other gyroharmonics.

Important findings from earlier work [Stubbe *et al.*, 1984] have been confirmed by the present experiments:

12. The DM (but not the 2DM) and the DP often possess

weaker upshifted mirror images (the UM and UP, respectively).

13. A strongly developed BUM is often accompanied by a secondary maximum at  $2\Delta f_{\text{BUM}}$ .

The characteristic variations in the anomalous absorption and SEE properties that we have seen in the figures above are due to the fact that we have systematically varied the pump frequency around a chosen gyroharmonic, while the ionosphere was in a stable and quiet state and showed little variability. In principle, corresponding experiments could also be performed with a fixed pump frequency, but a varying gyrofrequency. Indeed, there are times of day when the gyrofrequency in the interaction region changes in a systematic fashion. In the morning hours, when the  $F$  region falls from higher altitudes at night to lower altitudes at day, the gyrofrequency increases (and oppositely in the evening). Since the quantity of interest is  $\omega_0 - n\Omega_e$ , an increase in  $\Omega_e$  has a similar effect as a decrease in  $\omega_0$ . SEE experiments around sunrise, performed in 1985 without simultaneous absorption measurements [Leyser *et al.*, 1990], show corresponding changes in the SEE properties. Unfortunately, these authors were misled to attribute their findings to changes in the parameter  $\omega_{p0} - \omega_0$  (where  $\omega_{p0}$  is the plasmas frequency at the  $F$  layer maximum which increases with time around sunrise). The experiments reported in the present paper admit of no doubt that the controlling experimental parameter is  $\omega_0 - n\Omega_e$ , so that any other dependency which may exist will be of minor importance. Another statement by Leyser *et al.* [1990] that is not confirmed by our results is that, if not  $\omega_0 \approx \omega_{p0}$ , a strong DM will occur only in cases when the ionograms have wide and perturbed traces. Again, it depends predominantly on the choice of  $\omega_0 - n\Omega_e$  whether or not a strong DM is obtained. Given, as a reference, the pump frequency where the anomalous absorption (or equivalently the strength of the DM) has its minimum, the pump frequency of any of the other characteristic features (including a strongly developed DM) can be predicted with high precision, based on experimental experience. This should be a simplifying factor when it comes to theoretically understand the multiplicity of experimental features.

For a theoretical description it will be important to know whether all experimental features are causally interrelated and thus have to be treated in a unified way, or whether there are independent groups of features which may be treated separately. Naturally, the latter would considerably simplify the task. There is one important hint suggesting that we may be able to divide the features into two groups which, at least to a low order of description, are independent of each other. This hint stems from the fact that some of the features are "universal" (i.e., exist for all pump frequencies), whereas others exist only when  $\omega_0 \approx n\Omega_e$ . The latter will be termed here the "gyrofeatures." The main universal features are the anomalous absorption, SEE continuum and DM, whereas the main gyrofeatures are the BUM, DP, and BSS.

It appears plausible and is in correspondence with theoretical work [Mjølhus, 1993, and references therein], that the so-called universal features are physically connected with each other via the striations, excited by the pump. Linear mode conversion of the pump at the striations gives rise to upper hybrid waves which may then, by a process yet to be identified, produce secondary electromagnetic waves, showing their existence as SEE continuum and DM. Anomalous

absorption, in this picture, would be due to linear energy transfer from HF electromagnetic to HF electrostatic by the mode conversion process. Clearly, a weakening of the striations should lead to a corresponding weakening of the anomalous absorption, the SEE continuum and the DM.

If this physical picture should be correct, then any feature that does not disappear when the striations disappear cannot be physically connected with the universal features. The DP and BUM do not vanish when the universal features vanish. This is the point which most strongly supports the supposition that the universal features and the gyrofeatures may be treated separately. The situation is not quite as clear with regard to the BSS, because the range of existence of the BSS does not overlap with the frequency range occupied by the absorption and DM minimum. However, the fact that the BSS is a continuation of the DP (in the sense that the BSS begins to exist where the DP ceases to exist) speaks in favor of treating the BSS concurrently with the DP.

The primary question with regard to the universal features is why do the striations vanish (or, at least, are strongly reduced) at a certain pump frequency,  $\omega_{\min}$ , and how is  $\omega_{\min}$  related to  $n\Omega_e$ . Since  $\omega_{\min}$  serves as a natural reference frequency for the other features as well, it is particularly important to know whether or not  $\omega_{\min}$  is exactly given by  $n\Omega_e$ . This knowledge is also needed to evaluate the importance of cyclotron damping for any of the observed features. It is well known that, for a wave propagating nearly (but not exactly) perpendicular to the external magnetic field, cyclotron damping maximizes for  $\omega = n\Omega_e$ .

The primary question with regard to the gyrofeatures is why do these features exist only if  $\omega_0 \approx n\Omega_e$ , and what is the reason for the large qualitative differences between the case  $n = 3$  on the one hand, and the cases  $n = 4$  and  $n = 5$  on the other hand. A viable theory for the gyrofeatures has to meet the requirement that striations must not be involved, at least not as a crucial element. With regard to the BUM it must be shown that the mechanism in question generates only frequency upshifted electromagnetic waves. With regard to the BSS it must be shown that the mechanism in question generates frequency upshifted and downshifted electromagnetic waves of equal strength.

According to the discussion above, the excitation of striations, and their suppression at certain pump frequencies, should be central to a theoretical description of the universal features. *Mjøllhus* [1993], in extending earlier work on the generation of striations [e.g., *Vaskov and Gurevich*, 1977, 1984; *Grach et al.*, 1977; *Das and Fejer*, 1979; *Inhester*, 1982; *Dysthe et al.*, 1982], was able to show that the ability of striations to trap HF electrostatic waves is greatly reduced within a narrow pump frequency band slightly below a gyroharmonic. This, in turn, weakens the feedback mechanism that causes striation growth. While this theoretical approach as such appears very appealing, a quantitative estimate of the frequency bandwidth in which striation suppression occurs becomes very difficult because of the unknown importance of cyclotron damping. The reason why the latter is unknown is that the ratio  $k_{\parallel}/k_{\perp}$  (of the HF electrostatic waves) has a determining influence, but cannot be specified by any reasonable ad hoc assumption. Therefore a rather involved numerical analysis of the problem at hand appears unavoidable.

Given the existence of striations, the next question to be answered concerns the generation of the secondary electro-

magnetic waves which constitute the complex SEE phenomenon. For the universal SEE features, the source wave is likely to be an upper hybrid wave (UH), as excited by mode conversion of the pump at the striations (S),

$$\text{EM} + \text{S} \rightarrow \text{UH} \quad (1)$$

The upper hybrid wave may subsequently decay into an electromagnetic *O*-mode wave (propagating along the magnetic field) and a lower hybrid wave (LH),

$$\text{UH} \rightarrow \text{EM} + \text{LH} \quad (2)$$

and the EM wave may escape from the plasma to become observable on the ground. This mechanism was analyzed by *Murtaza and Shukla* [1984] and applied to the DM feature by *Leyser* [1991]. It was shown by *Stenflo and Shukla* [1992] that density gradients may significantly affect the properties of the LH waves. It must also be taken into consideration that, due to their large group velocities, the EM waves have a very short residence time in the interaction region, whereby the efficiency of mechanism (2) will be strongly reduced.

The disappearance of the DM at the pump frequency  $\omega_{\min}$  is explained by *Leyser* [1991] as being due to cyclotron damping of the UH waves when  $\omega_0 = n\Omega_e$ . This explanation is self-contradictory, because in the absence of UH waves striations cannot be excited, which in turn implies that UH waves will not be generated in the first place. Consequently, cyclotron damping effects should be primarily considered within a complete theory of striation formation, and not independently after assuming that a given striation level exists. A similar comment relates to the mechanism proposed by *Rao and Kaup* [1990]. These authors explain the disappearance of the DM in terms of linear conversion of propagating UH waves into nonpropagating EB (electron Bernstein) waves,  $\text{UH} \rightarrow \text{EB}$ . These EB waves are not able to decay into EM and LH [*Rao and Kaup*, 1990].

An alternative to (2) could be the decay process

$$\text{UH} \rightarrow \text{EB} + \text{LH} \quad (3)$$

with the possibility of subsequent mode converting scattering according to

$$\text{UH} + \text{LH} \rightarrow \text{EM} \quad (4)$$

or

$$\text{EB} + \text{LH} \rightarrow \text{EM} \quad (5)$$

or

$$\text{EB} + \text{S} \rightarrow \text{EM} \quad (6)$$

The frequency of the resulting electromagnetic waves is given by

$$\omega_{\text{EM}} = \omega_{\text{HF}} \pm \omega_{\text{LF}} \quad (7)$$

where HF denotes the high-frequency electrostatic waves (UH or EB) and LF denotes the low-frequency electrostatic perturbations (LH or S). Since  $k_{\text{EM}}$  is much smaller than  $k_{\text{HF}}$  and  $k_{\text{LF}}$ , the minus (plus) sign in (7) relates to HF and LF waves having the same (opposite) propagation directions.

Scattering processes of this kind were invoked by *Stubbe et al.* [1984] to explain several of the SEE features. How-

ever, the high- and low-frequency electrostatic waves employed were assumed to be Langmuir waves (L) propagating at small angles to the external magnetic field and ion acoustic waves (IA). This assumption was made because incoherent scatter experiments had indicated that these waves are strongly excited by the parametric decay instability  $EM \rightarrow L + IA$ . Since these waves are not subject to cyclotron damping, they should not vanish near gyroharmonics. This implies that only the continuum that remains when the DM is suppressed at  $\omega_{\min}$  (see Figure 1, panel c; Figure 2, panel d; Figure 3, panel c) could be due L and IA waves.

The advantage of the combined processes (3) to (6) over (2) is that the rapid propagation of the resulting EM wave out of the interaction region has no adverse effect, since the EM wave is not actively involved in processes (3) to (6). An analysis of SEE features based on these processes has not been performed in the literature thus far. We mention in passing that one would obtain EM waves with frequencies  $\omega_{EM} = \omega_0 \pm \omega_{LH}$  from (3), (4),  $\omega_{EM} = \omega_0 - 2\omega_{LH}$  (and  $\omega_{EM} = \omega_0$ ) from (3), (5), and  $\omega_{EM} = \omega_0 - \omega_{LH}$  from (3), (6).

Turning now to the so-called gyrofeatures, we have to rely on processes that do not crucially depend on the existence of striations (and of UH waves generated by linear mode conversion at the striations). As explained above, this is due to the fact that two of the gyrofeatures (BUM and DP) exist in strongly developed form at pump frequencies where striations are suppressed. Regarding the third gyrofeature (the BSS), explanations involving striations cannot be ruled out since this feature exists at pump frequencies where striations are present. However, the strong connection which is observed to exist between the DP and the BSS suggests that these two features should be treated concurrently.

A process which is likely to be important in the given context is the decay

$$EM \rightarrow EB + LH \quad (8)$$

which was analyzed by *Tripathi and Liu* [1993]. These authors apply process (8), in conjunction with (4), to explain the BUM feature. It is assumed that the LH wave in (4) is generated by (8) and that the UH wave in (4) is generated by (1). The proposed mechanism thus requires striations and, for the reasons given above, does not appear appropriate therefore. Another difficulty with this explanation is that symmetric sidebands are predicted, given by  $\omega_{EM} = \omega_0 \pm \omega_{LH}$ , whereas the observed BUM feature is entirely upshifted. It is argued by *Tripathi and Liu* [1993] that the lower sideband waves  $\omega_{EM} = \omega_0 - \omega_{LH} = \omega_{EB}$  are suppressed by cyclotron damping, because  $\omega_{EB} \approx n\Omega_e$ . However, the same argument might be applied to the upper sideband  $\omega_{EM} = \omega_0 + \omega_{LH} = 2\omega_0 - \omega_{EB}$ . In addition, the frequency width of the BUM is much too large (see Figures 1 and 2) for a suppression of the complete downshifted counterpart of the BUM to be possible by cyclotron damping. *Goodman et al.* [1993] offer the same two-step process, consisting of (8) and (4), as an explanation of the BUM. These authors do not at all address the question of why a symmetric mechanism should generate an asymmetric spectrum. Yet it is just this spectral asymmetry which represents the major problem in explaining the BUM, and a theory of the BUM cannot therefore avoid this question.

*Kuo* [1992] discusses the decay of a standing Bernstein wave into an electromagnetic wave and a lower hybrid wave

$$EB \rightarrow EM + LH \quad (9)$$

and applies this process to the BSS. The problem with regard to (9) is the same as it was with regard to (2). Namely, the short residence time,  $\tau$ , of the EM wave in the interaction region will severely limit the efficiency of processes (9) and (2). *Kuo* [1992] estimates  $\tau$  to be of the order of 10  $\mu s$ . This time appears much too short for EM waves to grow from the noise level to the levels observed in SEE experiments.

The DP has been tentatively explained in terms of the mode-converting scatter process  $L + IA \rightarrow EM$ , taking place at the first Airy maximum where the L and IA waves are, supposedly, most strongly excited [*Stubbe et al.*, 1984]. This idea has been elaborated by *Leyser and Thidé* [1988] where the density structure caused by the standing pump wave has been taken into consideration. The experimental facts that the DP is a gyrofeature and that  $\Delta f_{DP}$  depends sensitively on  $f_0$  (see Figures 3, 9, and 10) rules out these explanations. Furthermore, it is predicted by *Leyser and Thidé* [1988] that  $\Delta f_{DP}$  should depend on pump power. Experiments performed in 1989 (where the pump power has been systematically changed while the DP was monitored) showed that only the strength of the DP depends on pump power, but not its frequency. This again rules out the above explanation.

*Dimant et al.* [1992] have shown that electron acceleration by HF plasma turbulence will be intensified when the turbulence frequency is in the gyroharmonics range. It is argued that the resulting changes occurring in the electron distribution function may be responsible for some of the changes seen in the SEE spectra. A concrete relationship between electron acceleration and defined SEE properties has, however, not been established.

We have to come to the unfortunate conclusion that hardly any of the experimental features discussed in the present paper is satisfactorily explained by existing theoretical work. Many of the elementary processes treated in the literature may however prove to be useful when embodied in a comprehensive theoretical concept which aims at coping with the full experimental reality, rather than selected facets of it.

**Acknowledgments.** We wish to thank Helmut Gegner for keeping the heating facility in excellent working condition, and for his diligent operation of the facility during these experiments. The Heating project has been financially supported by the Deutsche Forschungsgemeinschaft (DFG). Two of us (A.S. and F.H.) were supported by S.E.R.C. grant GR/H/32025 during the course of this work.

The Editor thanks E. Mjølhus for his assistance in evaluating this paper.

## References

- Das, A. C., and J. A. Fejer, Resonance instability of small-scale field-aligned irregularities, *J. Geophys. Res.*, **84**, 6701–6704, 1979.
- Dimant, Ya. S., A. V. Gurevich, and K. P. Zybin, Acceleration of electrons in the ionosphere under the action of intense radio-waves near electron cyclotron harmonics, *J. Atmosph. Terr. Phys.*, **54**, 425–436, 1992.
- Dysthe, K. B., E. Mjølhus, H. Pécseli, and K. Rypdal, Thermal cavitons, *Phys. Scr.*, **T2/2**, 548–559, 1982.
- Goodman, S., B. Thidé, and L. Erukhimov, A combined parametric

- and conversion mechanism for upshifted stimulated electromagnetic emissions, *Geophys. Res. Lett.*, *20*, 735–738, 1993.
- Grach, S. M., A. N. Karashtin, N. A. Mityakov, V. O. Rapoport, and V. Yu. Trakhtengerts, Parametric interaction between electromagnetic radiation and the ionospheric plasma, *Radio Phys. Quantum Electron.*, *20*, 1254–1258, 1977.
- Graham, K. N., and J. A. Fejer, Anomalous radio wave absorption due to ionospheric heating effects, *Radio Sci.*, *11*, 1057–1063, 1976.
- Inhester, B., Thermal modulation of the plasma density in ionospheric heating experiments, *J. Atmos. Terr. Phys.*, *44*, 1049–1059, 1982.
- Jones, T. B., T. Robinson, P. Stubbe, and H. Kopka, A hysteresis effect in the generation of field-aligned irregularities by a high-power radio waves, *Radio Sci.*, *18*, 831–834, 1983.
- Jones, T. B., T. Robinson, P. Stubbe, and H. Kopka, Frequency dependence of anomalous absorption caused by high-power radio waves, *J. Atmos. Terr. Phys.*, *46*, 147–153, 1984.
- Kopka, H., P. Stubbe, T. B. Jones, and T. Robinson, Nonlinear reflectivity of high-power radio waves in the ionosphere, *Nature*, *295*, 680, 1982.
- Kuo, S. P., Parametric excitation of electromagnetic waves by electron Bernstein waves, *Phys. Fluids B*, *4*, 4094–4100, 1992.
- Leyser, T. B., Parametric interaction between upper hybrid and lower hybrid waves in heating experiments, *Geophys. Res. Lett.*, *18*, 408–411, 1991.
- Leyser, T. B., and B. Thidé, Effect of pump-induced density depletions on the spectrum of stimulated electromagnetic emissions, *J. Geophys. Res.*, *93*, 8681–8688, 1988.
- Leyser, T. B., B. Thidé, H. Derblom, Å. Hedberg, B. Lundborg, P. Stubbe, and H. Kopka, Dependence of stimulated electromagnetic emission on the ionosphere and pump wave, *J. Geophys. Res.*, *95*, 17,233–17,244, 1990.
- Mjølhus, E., On linear conversion in a magnetized plasma, *Radio Sci.*, *25*, 1321–1339, 1990.
- Mjølhus, E., On the small scale striation effect in ionospheric radio modification experiments near harmonics of the electron gyro frequency, *J. Atmos. Terr. Phys.*, *55*, 907–918, 1993.
- Murtaza, G., and P. K. Shukla, Nonlinear generation of electromagnetic waves in a magnetoplasma, *J. Plasma Phys.*, *31*, 423–436, 1984.
- Rao, N. N., and D. J. Kaup, Upper hybrid mode conversion and resonance excitation of Bernstein modes in ionospheric heating experiments, *J. Geophys. Res.*, *95*, 17,245–17,252, 1990.
- Stenflo, L., and P. K. Shukla, Generation of radiation by upper-hybrid waves in non-uniform plasmas, *Planet. Space Sci.*, *40*, 473–476, 1992.
- Stocker, A. J., F. Honary, T. R. Robinson, T. B. Jones, and P. Stubbe, Anomalous absorption during artificial modification at harmonics of the electron gyrofrequency, *J. Geophys. Res.*, *98*, 13,627–13,634, 1993.
- Stubbe, P., and H. Kopka, Stimulated electromagnetic emission in a magnetized plasma: A new spectral feature, *Phys. Rev. Lett.*, *65*, 183–186, 1990.
- Stubbe, P., H. Kopka, T. B. Jones, and T. Robinson, Wide band attenuation of radio waves caused by powerful HF waves: Saturation and dependence on ionospheric variability, *J. Geophys. Res.*, *87*, 1551–1555, 1982.
- Stubbe, P., H. Kopka, B. Thidé, and H. Derblom, Stimulated electromagnetic emission: A new technique to study the parametric decay instability in the ionosphere, *J. Geophys. Res.*, *89*, 7523–7536, 1984.
- Thidé, B., H. Kopka, and P. Stubbe, Observations of stimulated scattering of a strong high-frequency radio wave in the ionosphere, *Phys. Rev. Lett.*, *49*, 1561–1564, 1982.
- Tripathi, V. K., and C. S. Liu, O mode decay and upshifted electromagnetic emissions near cyclotron harmonics in the ionosphere, *J. Geophys. Res.*, *98*, 1719–1723, 1993.
- Utlaut, W. F., and E. F. Violette, A summary of vertical incidence radio observations of ionospheric modification, *Radio Sci.*, *9*, 895–903, 1974.
- Vaskov, V. V., and A. V. Gurevich, Resonance instability of small-scale plasma perturbations (in Russian), *Zh. Eksp. Teor. Fiz.*, *73*, 923–936, 1977. (*Sov. Phys. JETP*, Engl. Transl., *46*, 487–494, 1978.)
- Vaskov, V. V., and A. V. Gurevich, Amplification of resonant instability and generation of wideband radio emission by high-power radio waves incident on the ionosphere, *Geomagn. Aeron.*, *24*, 350–356, 1984.
- F. Honary, T. B. Jones, T. R. Robinson, and A. J. Stocker, Department of Physics and Astronomy, Leicester University, Leicester, LE1 7RH, United Kingdom. (e-mail: JANET.fah@uk.ac.le.ion)
- P. Stubbe, Max-Planck-Institut für Aeronomie, Postfach 20, D-37189 Katlenburg-Lindau, Germany. (e-mail: Internet. stubbe@linmpi.dnet.gwdg.de)

(Received June 23, 1993; accepted December 23, 1993.)